JOURNAL OF MATERIALS SCIENCE 25 (1990) 4331–4340

Slip casting of Al_2O_3 and Al_2O_3/ZrO_2 composites

A. BELLOSI, C. GALASSI, S. GUICCIARDI
Research Institute for Ceramics Technology, National Research Council, Faenza, Italy

Al_2O_3 and Al_2O_3/ZrO_2 composites have been fabricated by slip casting from aqueous suspensions. The physical and structural characteristics of the starting powders, composition of the suspensions, casting behaviour, microstructure of the green and fired bodies and the mechanical properties of the products were investigated. The addition of ZrO_2 to Al_2O_3 leads to a significant increase in fracture toughness when ZrO_2 particles are retained in the tetragonal form (transformation-toughening mechanism) but when microcracking (due to the spontaneous transformation of ZrO_2 from the tetragonal phase to the monoclinic one) is dominant, an excellent toughness value is accompanied by a drastic drop in strength and hardness.

1. Introduction

Slip casting is a well-established ceramic fabrication technique suitable for producing rather complex shapes. The use of slip casting into plaster moulds for shaping toughened ceramics has been reported [1, 2]. Lange *et al.* [3–6], in considering the choice of the forming technique, have emphasized the importance of avoiding the detrimental presence of zirconia agglomerates which can leave crack-like voids around them, thereby decreasing material strength. Slip casting generally employs aqueous suspensions and agglomeration is avoided by proper dispersion of the powders in water. The development of a well dispersed and stable suspension is a necessary step for the slip-casting process. An additional factor to be controlled when casting zirconia-toughened alumina is the dispersion of the two types of powders with different surface properties and different physical characteristics. Claussen and co-workers [7–9] studied the toughening mechanisms of alumina with the addition of ZrO_2. Recently, it has been verified [10–12] that when m- and t-ZrO_2 are present, the microcracking mechanism must be added to the stress-induced transformation. Strength and toughness depend on many parameters: the amount of ZrO_2, particle size and shape, particle size distribution, zirconia particle location (intergranular or intragranular). This investigation aims at the optimization of the compositions of suspensions for slip casting into plaster mould using a powder mixture containing 30 wt % zirconia (t-3 mol % Y_2O_3), that had proved to be a good compromise between strength and toughness in the production of substrates [13]. For a comparison, unstabilized and partially stabilized ZrO_2 were tested, the latter with high and low specific surface area. Characteristics of the starting powders, casting behaviour, microstructure of the cast and fired bodies, and mechanical properties of the products, were correlated.

2. Experimental procedure

2.1. Materials

Experiments were carried out with the following starting mixtures.

System A: 70 wt % Al_2O_3 (Alcoa A16 S.G., Aluminium Co. of America, Pittsburg, Pennsylvania) + 30 wt % ZrO_2 (Toyosoda TZ 3Y-S, Toyo Soda NFG Co., Tokyo, Japan) (t-ZrO_2 + 3 mol % Y_2O_3, 7.8 $m^2 g^{-1}$).

System B: 70 wt % Al_2O_3 + 30 wt % ZrO_2 (Toyosoda TZ 3Y, Toyo Soda NFG Co., Toyko, Japan) (t-ZrO_2 + 3 mol % Y_2O_3, 18.5 $m^2 g^{-1}$).

System C: 70 wt % Al_2O_3 + 30 wt % ZrO_2 (Harshaw Spec. 102, The Harshaw Chem. Co., Cleveland, Ohio) (m-ZrO_2, 28 $m^2 g^{-1}$).

System D: Al_2O_3 (10.2 $m^2 g^{-1}$).

Two tetragonal ZrO_2 powders (3 mol % Y_2O_3) (A and B) and one type of ZrO_2 monoclinic (C) were employed to evaluate (i) the influence of the specific surface area on the casting behaviour and on the properties of green and fired bodies, (ii) the effect on toughness and strength of zirconia with different crystalline phases and different grain size, and (iii) the degree of agglomeration during the forming process and the grade of retention of tetragonal particles during cooling after sintering and their influence on microstructure and mechanical properties of the products.

2.2. Casting tests

The casting suspensions were prepared by dispersing the powders in a mill using ZrO_2 balls for 20 min fast stirring in water to which a deflocculating agent had been added. Some preliminary tests were carried out to evaluate different dispersants for Al_2O_3 and Al_2O_3/ZrO_2 mixtures, and it was decided to work with an aqueous suspension more acceptable to slip casting than other dispersants. Among the various suspensions tested, a sodium ligninsulphonate-based deflocculant (Vanisperse CBF, Borregaard) was chosen, considering the good results obtained during preliminary experiments and in the casting of other ceramic powders [14]. It resulted in a stable suspension, with a high percentage of the suspended solid phase. The pH of all tested systems ranged between 9.9 and 11.4. In Table I details of the experiments are shown. After evacuation of the slips, the kinetics of the slip casting

0022–2461/90 $03.00 + .12

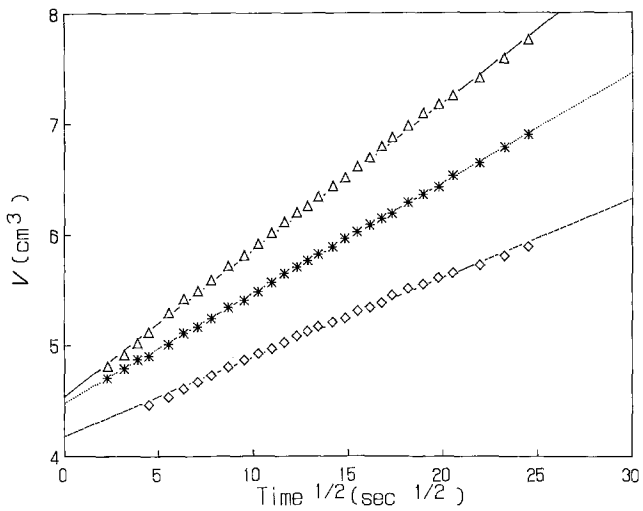

Figure 1 Variation of the volume of the water absorbed by the mould with the square root of time, for system D with constant amount of deflocculant, varying solid-phase content (△) 37 vol %, (*) 43 vol %, (◇) 50 vol %.

was evaluated using an apparatus proposed by Celik *et al.* [15–17], designed to determine the water-removal rate by the mould from the slip. All casting measurements were carried out using moulds with a plaster/water weight ratio 100:64, with the above-mentioned apparatus. The casting kinetics is usually simply described by the relationship

$$L^2 = K_0 \Delta P t = K_1 t$$

where L is the cast thickness at time t, K_0 is termed the casting constant and is related to the permeability of the cast, the volume fraction of solid in the suspension and the suction pressure of the mould, ΔP, that is constant during the experiment [15]. Assuming that the cast produced is of constant density through its thickness, that L is proportional to V, the volume of water removed from the suspension, and the above equation can be adapted to the experimental evaluation of the volume of water absorbed (V) at time (t) by the following relation [15]

$$V = V_0 + Kt^{1/2}$$

where V_0 is the initial value of V related to the air gap present above the suspension, K (m sec$^{-1/2}$) is a constant normalized to the unit area of the mould–slip interface. A plot of V against $t^{1/2}$ is linear after the stage of filling the gap between the slip and the mould (Fig. 1 shows plots for system D, for three different fractions of solid in the suspension). The constant K experimentally measured with this method is directly related to the volume of water absorbed by the mould and it can be considered an indirect measure of the casting rate of the slip because, assuming a constant suction pressure of the mould, for fixed values of solid phase, K depends only on the permeability of the cast. For casts with low permeability (low constant), longer times are necessary for obtaining a fixed thickness. The solid phase content strongly influences the value of the constant, because for a low quantity of solid phase more water must be extracted from the slip to obtain a fixed thickness but the permeability of the cast in this case is higher, therefore the constant increases. In the following sections the constant K will be called the casting constant for its relation with K_1.

TABLE I Slip casting conditions, casting behaviour and characteristics of green and sintered samples

	Batch composition			Casting behaviour		After casting		After sintering		
	Solid (wt %)	Solid (vol %)	Deflocculant (wt ‰)	pH	Casting rate, K (10^{-5} m sec$^{-1/2}$)	Green density (g cm^{-3})	Relative green density (%)	Final density (g cm^{-3})	Relative final density (%)	Shrinkage (%)
A	70	34	6.0	11.2	4.69	2.50	56.3	4.41	99.3	17
	75	40	5.0	11.2	3.78	2.48	55.8			
	75	40	6.0	11.3	3.55	2.49	56.1			
	75	40	7.0	11.4	4.61	2.52	56.7			
B	70	34	5.0	11.2	5.37	2.39	53.8	4.39	98.9	19
	70	34	6.0	10.8	4.85	2.41	54.3			
	70	34	7.0	10.7	7.69	2.46	55.4			
C	70	35	6.0	10.8	4.32	2.70	61.9	4.30	98.6	16
	75	41	6.0	10.6	3.81	2.71	62.1			
	80	48	6.0	10.5	2.32	2.73	62.6			
	80	48	5.0	10.5	1.99	2.76	63.3			
	80	48	7.0	10.8	3.08	2.68	61.5			
D	70	37	6.0	10.0	5.52	2.44	60.7	3.95	99.0	15
	75	43	6.0	10.0	4.15	2.45	61.4			
	80	50	6.0	10.0	2.99	2.58	64.7			
	80	50	5.0	9.9	–	2.44	61.2			
	80	50	7.0	10.0	2.77	2.48	62.2			
	80	50	8.0	10.2	4.39	2.41	60.4			

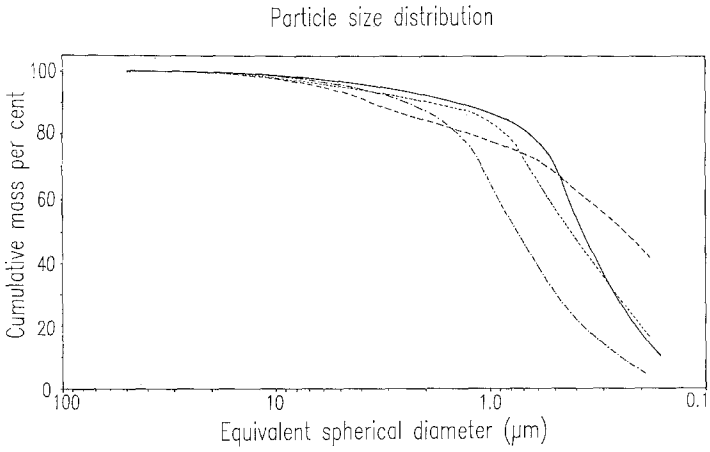

Figure 2 Cumulative mass curves of the tested mixtures Al_2O_3/ZrO_2 (systems (——) A, (– – –) B and (—·—) C) and of Al_2O_3 ((– – – –) system D).

2.3. Characterization of cast and fired bodies

All the cast samples were presintered at 1100° C to obtain a sufficient strength for mechanical machining and finishing. Final sintering of zirconia-toughened alumina was performed at $T = 1650°$ C for 120 min, of alumina at 1600° C for 30 min. These parameters were chosen on the basis of the final densities obtained after preliminary trials. Bulk densities of as-cast and sintered bodies were measured according to the mercury-displacement technique. An evaluation of the particle packing and of the distribution of open porosity in green samples was carried out using a porosimeter (mercury intrusion) (Porosimeter series 2000, C. Erba Instruments), and scanning electron microscope (SEM) (Autoscan, ETEC Corporation) analysis of as-cast pieces. The linear shrinkage of the samples after sintering was determined. Microstructural evaluation of fracture surfaces and of casting surfaces were performed on sintered materials. Flexural strength (Instrom, Universal Testing Machine mod.1195, Canton, Mississippi) of selected compositions was measured by the three-point bend method, with 28 mm span and a cross-head speed of 0.5 mm min^{-1} (size of the sample 4 × 3 × 32 mm^3). The critical stress intensity factor (K_{IC}) values were determined using the indentation technique developed by Evans and Charles [18]. The Vickers microhardness (Zwick 3212 microdurometer) was measured with a 500 g

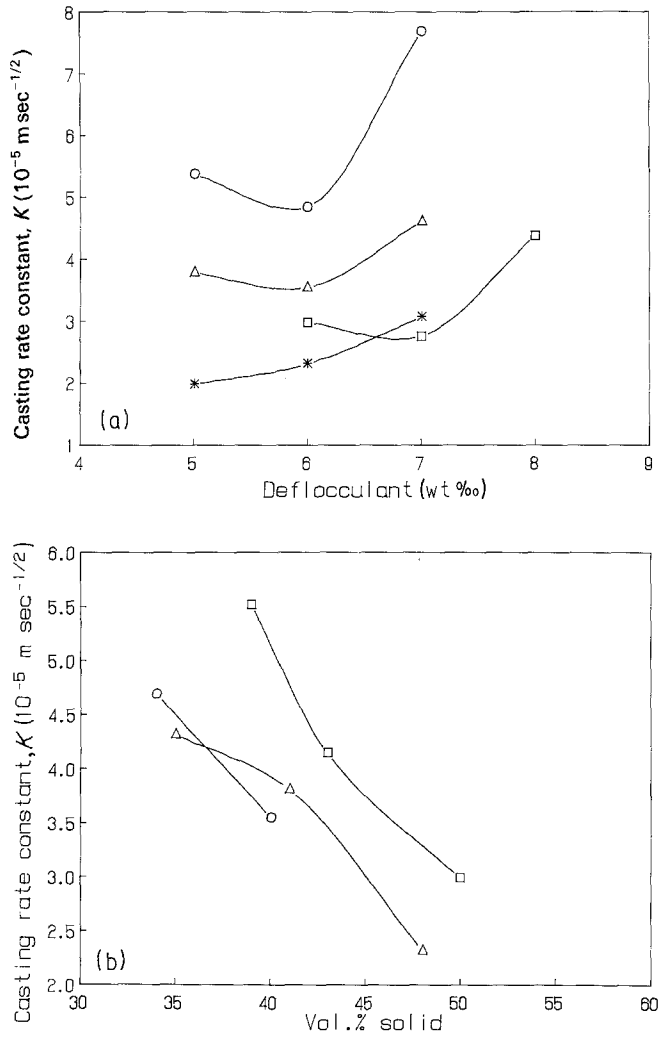

Figure 3 Casting rate constant plotted against: (a) deflocculant concentration (△) A, 40 vol % solid; (○) B, 34 vol % solid; (*) C, 48 vol % solid; (□) D, 50 vol % solid and (b) solid-phase content (○) A, (△) C, (□) D, 6 wt % deflocculent, for the various systems tested.

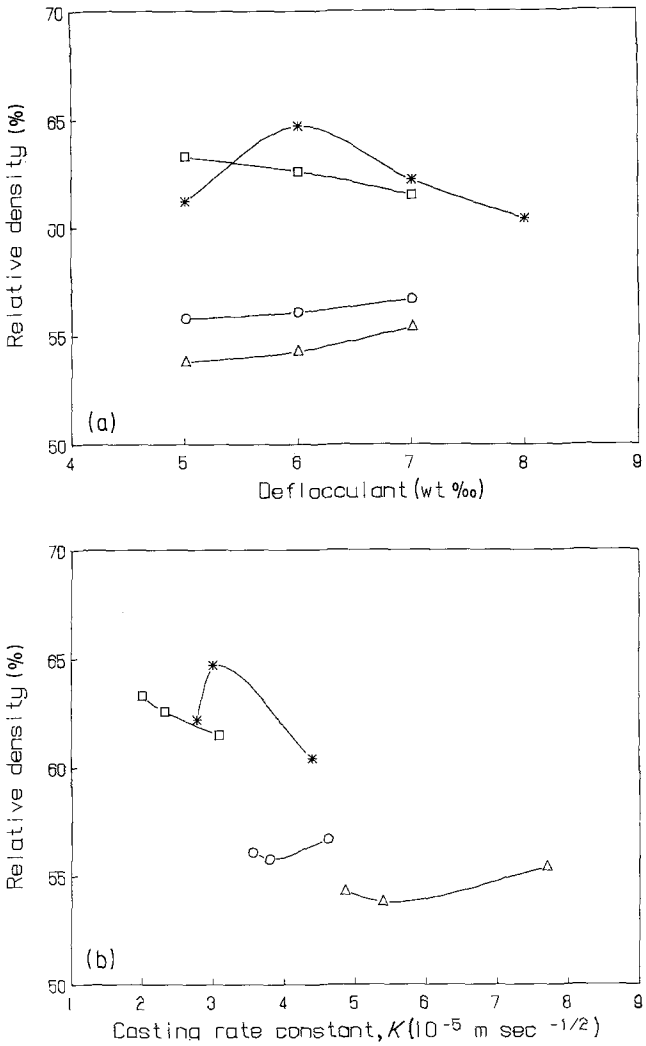

Figure 4 Green density values plotted against (b) casting rate constants, and (a) deflocculant concentration, for the various systems tested. (○) A, 40 vol % solid; (△) B, 34 vol % solid; (□) C, 48 vol % solid; (*) D, 50 vol % solid.

load, loading rate below 0.3 mm sec^{-1}, indentation time 10 sec.

3. Results and discussion

3.1. Powder characterization and dispersion

Control of particle size and shape of the starting powders is a primary factor in the casting behaviour of the suspension. Table II shows some microstructural parameters of the starting powders. The morphology of the particles at SEM analysis is essentially rounded for all the tested powders and the agglomeration grade is very low. Comparing the size of the agglomerates of the mixtures by the Sedigraph, after ultrasonic dispersion, Fig. 2, system C appears the most agglomerated.

3.2. Casting behaviour

From the data reported in Table I it can be concluded that castable suspensions with the highest solid-phase content are obtained when using only alumina (D) (50 vol %): the addition of zirconia lowers this value (40 vol % for A, 34 vol % for B, 48 vol % for C). On increasing the amount of solid phase the suspensions were not castable. Figs 3a and b show the casting rate constants (K) plotted against the deflocculant concentration and the solid-phase content, respectively, of the different systems. The variations of K with the amount of deflocculant show approximately the same trend for the various systems: an increase in the casting rate constant occurs at the higher deflocculant concentration tested, while a slight variation is detected in the lower range of deflocculant concentration. A shift of the plots (Fig. 3a) is shown in agreement to the solid-phase content: from high values of casting rate constants in correspondence with low solid-phase contents, to low K values on increasing the solid-phase content; this behaviour is confirmed from the data in Fig. 3b. The deflocculation effectiveness can be detected only over a narrow range of concentration (from 5 to 7 wt ‰, for Al_2O_3/ZrO_2 systems and from 5 to 8 wt ‰ for the Al_2O_3 system); for values of concentration outside the quoted ranges, the mixture is not castable. The best results for the slip casting of Al_2O_3/ZrO_2 systems can be indicated at a deflocculant concentration of 6 wt ‰, with solid phase content

TABLE II Starting powder characteristics

Powder	Specific surface area, BET ($m^2 g^{-1}$)	Equivalent spherical diameter (μm)	Particle size, SEM (μm)	Y_2O_3 (wt %)	Crystalline phases
Al_2O_3*	10.2	0.073	0.5–1.0	–	α-Al_2O_3
ZrO_2†	18.5	0.054	0.2–0.5	5.03	t-ZrO_2
ZrO_2‡	7.8	0.129	0.5	5.27	t-ZrO_2
ZrO_2§	28	0.036	0.4	–	m-ZrO_2

*Al_2O_3 A-16 S.G. Alcoa.
†ZrO_2 TZ-3Y Toyosoda.
‡ZrO_2 TZ-3YS Toyosoda.
§ZrO_2 Harshaw spec. 102.

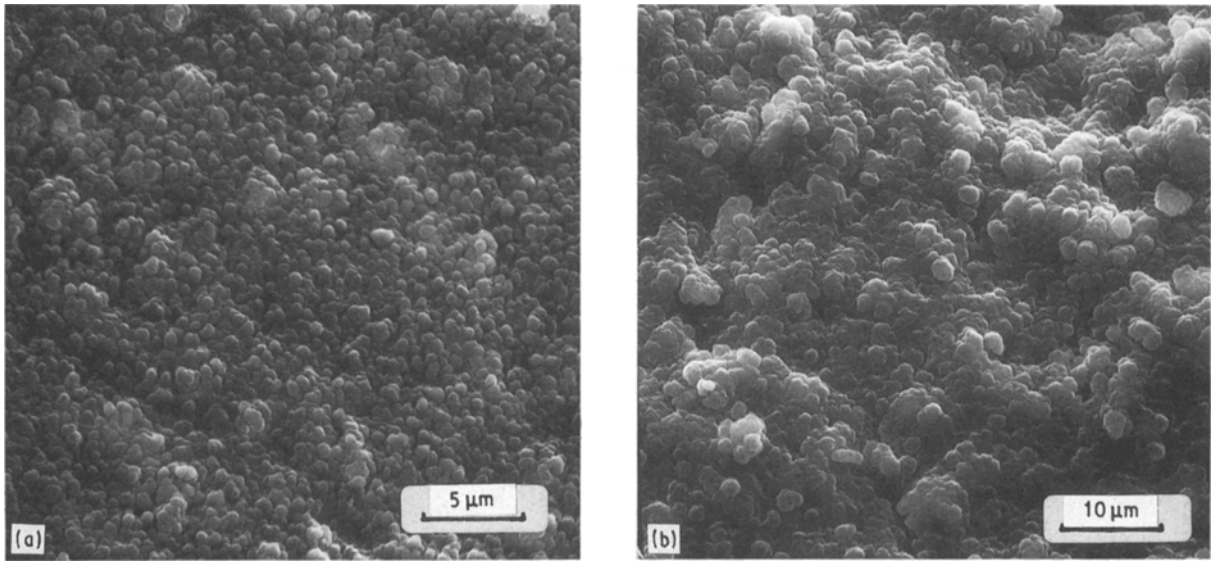

Figure 5 Scanning electron micrographs of the fracture surface of green bodies for: (a) system D, and (b) system B.

varying according to the physico-chemical characteristics of ZrO_2, while for Al_2O_3 the optimal deflocculant concentration is 7 wt‰.

The relative densities of the cast bodies are related to the deflocculant concentration and to the casting rate constants (Figs 4a and b, respectively). At higher solid-phase contents (C and D) an inverse relationship exists between relative green density and K and/or deflocculant concentration, while for the systems castable with lower solid-phase content (A and B) an increase in density occurs, increasing the above parameters. The linear shrinkage changes slightly for the various systems. Components of large dimensions did not warp during sintering.

3.3. Characterization of cast samples

3.3.1. Microstructure of green bodies

Using Al_2O_3 only (D), the microstructure of green bodies shows well-packed particles, without aggregates or defects (Fig. 5a). When ZrO_2 was present, porosity and cracks were present (in Fig. 5b an example is shown of system B); no visible differences were observed between samples containing different types of ZrO_2. The distribution of zirconia particles in the green bodies was irregular and aggregates are shown, for example (Figs 6a, b), irrespective of the characteristics of the starting zirconia. An important parameter is the pore size distribution of the cast body, which is affected by many variables: composition of the mixtures, casting behaviour, drying rate, particle characteristics, but particle and aggregate size distribution play the major role for a good slip. The distribution of the open porosity against pore radius of the as-cast samples (Fig. 7) indicates a similar behaviour for systems A and B in the region of low pore size (up to 0.03 μm), while a slightly higher presence of larger pores occurs when ZrO_2 with low specific surface area is employed. The addition of zirconia with the highest specific surface area (C) results in a small porosity with pore size ranging from

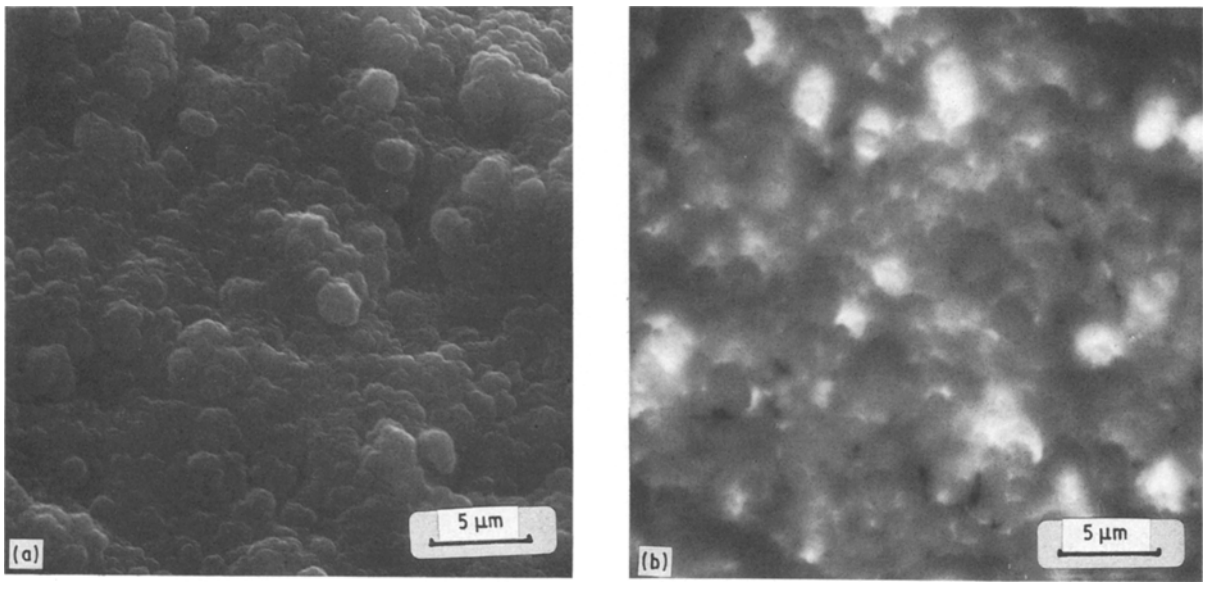

Figure 6 Scanning electron micrographs of fracture surface of a system B green sample: (a) morphology, (b) back-scattered electron image, showing the distribution and the aggregation state of ZrO_2 particles (white areas).

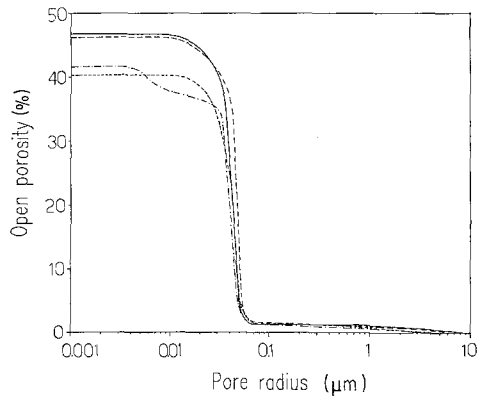

Figure 7 Cumulative curves (open porosity against pore radius) of the as-cast bodies.

0.005 to 0.3 μm, due to the good packing resulting from the very fine particles. However, in terms of green density, the best final result is achieved when casting alumina only.

3.3.2. Microstructure of fired bodies

An SEM analysis of the sintered surface which has not been in contact with the mould shows that very fine particles have segregated on a thin surface layer. For mixture A (Fig. 8), where Al_2O_3 is the finer powder, the surface shows little presence of ZrO_2; in the case of mixture B (Fig. 9), where both Al_2O_3 and ZrO_2 have about the same value of specific surface area, an amount of ZrO_2 corresponding to its percentage in the mixture, can be detected on the surface. In the sample obtained from C (Fig. 10), where ZrO_2 has the highest specific surface area, zirconia predominates on the surface. This could be explained on the basis of a fast particle deposition resulting from surface tension, following the draining of the excess slip. This behaviour is limited only to the very narrow layer close to the surface. The fractographs of the sintered samples do not show this layer (see, for example, Figs 11a, b and 12a, b, relative to B and C, respectively). As mentioned, zirconia particles aggregate during slip formation and ZrO_2 aggregates are retained after sintering [19, 20]. The coalescence and distribution of zirconia particles seem to be linked to the specific surface area of the starting powder: the best dispersion of ZrO_2 in the matrix is observed for A (ZrO_2 with low specific surface area), while in materials from B and C many clusters are present. The dispersion grade of zirconia particles also affects the porosity, which is higher for C (Figs 13a and b), corresponding to a more pronounced aggregation of ZrO_2. In all cases, the temperature and soaking time needed to achieve high density after sintering indicate that zirconia acts as a sintering inhibitor for alumina; the same behaviour has been observed by Wilfinger and Cannon [1]. Majumdar *et al.* [19] observed a reduction of the densification rate of Al_2O_3 by small additions of zirconia. Among the possible explanations for the changes in the densification behaviour, it appears [19] that the most promising lies in some involvement of solid solution effect and transport processes, most probably at grain boundaries. After sintering, when tetragonal zirconia is employed (A and B), ZrO_2 is retained in the tetragonal form in amounts of about 90%, while starting from m-ZrO_2 (C), about 90% ZrO_2 transforms from tetragonal to monoclinic.

3.4. Mechanical properties

The results of mechanical tests are shown in Table III. As expected, hardness, strength and the critical stress intensity factor are sensitive to the ZrO_2 particle size and crystalline form and to grain-size distribution. A slight reduction of hardness, with reference to Al_2O_3 material, is detected for composites A and B, while a remarkable drop in hardness is due to the presence of monoclinic zirconia (C). These samples were so heavily cracked during cooling by spontaneous transformation from tetragonal to monoclinic that they generally did not survive the sectioning process. Those that did survive had very low strength. On the contrary, the highest value of K_{IC} obtained for this composition, containing m-ZrO_2, confirms that microcracking plays an important role as toughening mechanism. For compositions A and B where the stress-induced

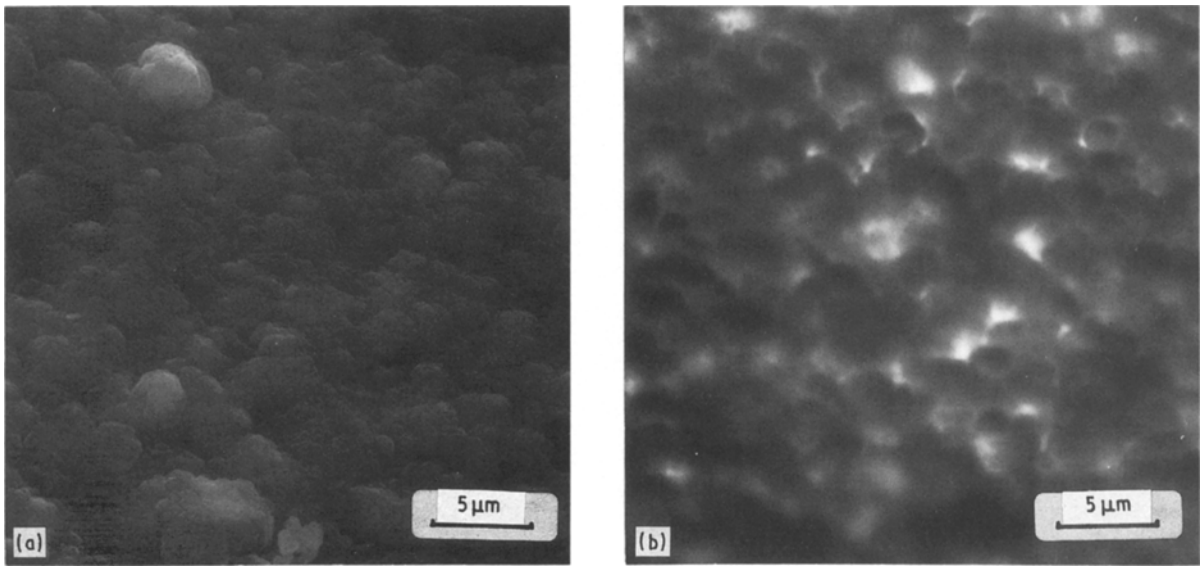

Figure 8 Scanning electron micrographs of the as-cast surface, for system A, showing little presence of ZrO_2 (white areas in b).

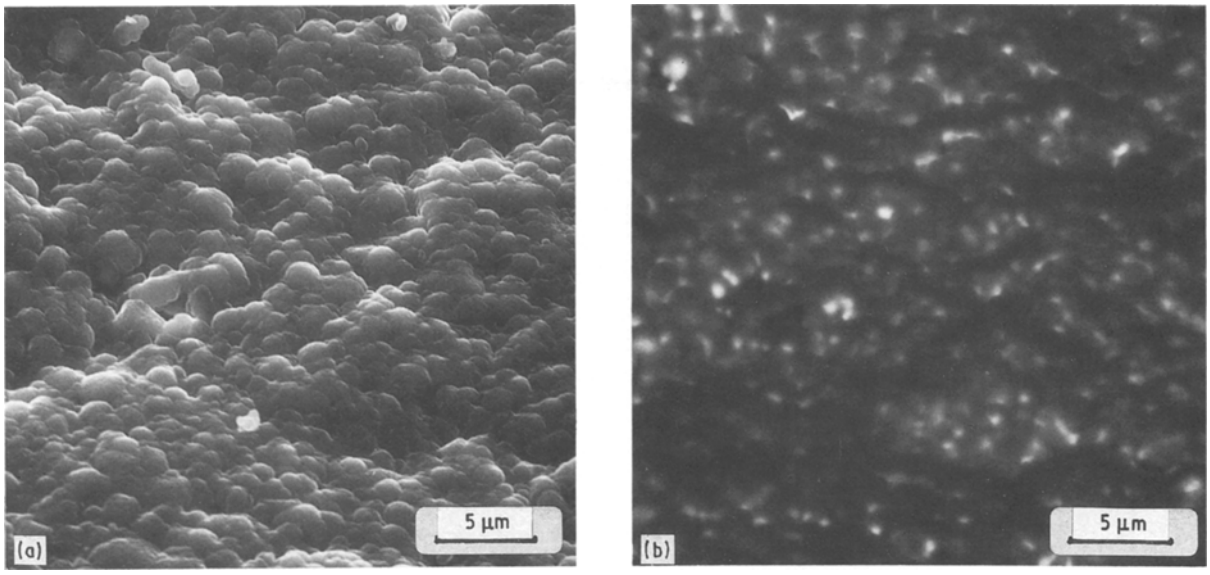

Figure 9 Scanning electron micrographs of the as-cast surface for system B, showing the presence and distribution of ZrO_2 (white areas in b).

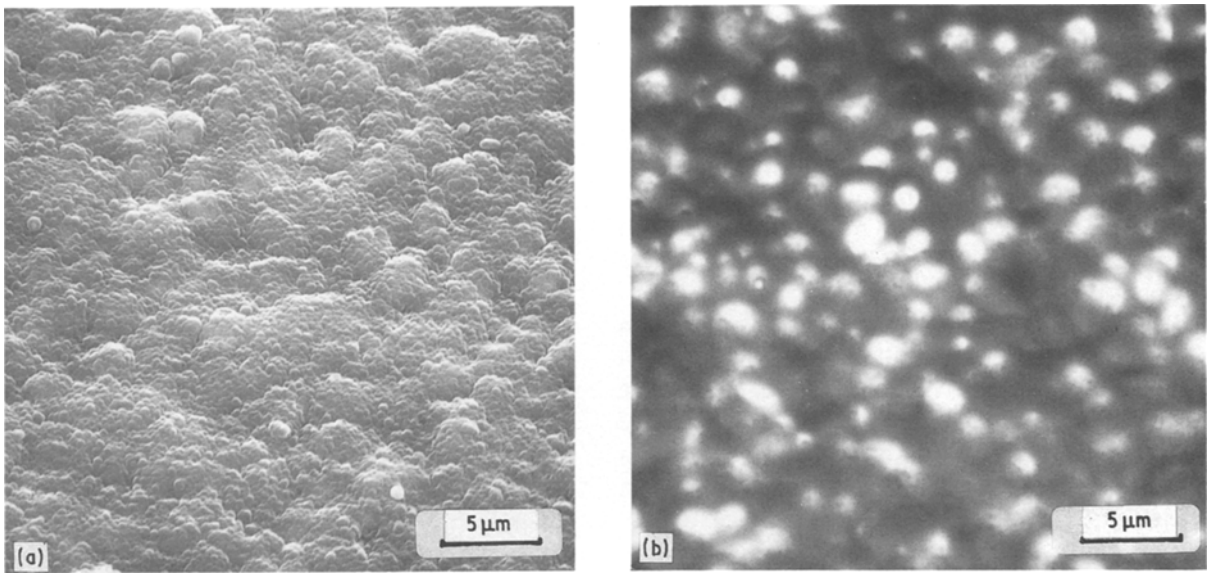

Figure 10 Scanning electron micrographs of the as-cast surface for system C, showing the presence of ZrO_2 (white areas in b).

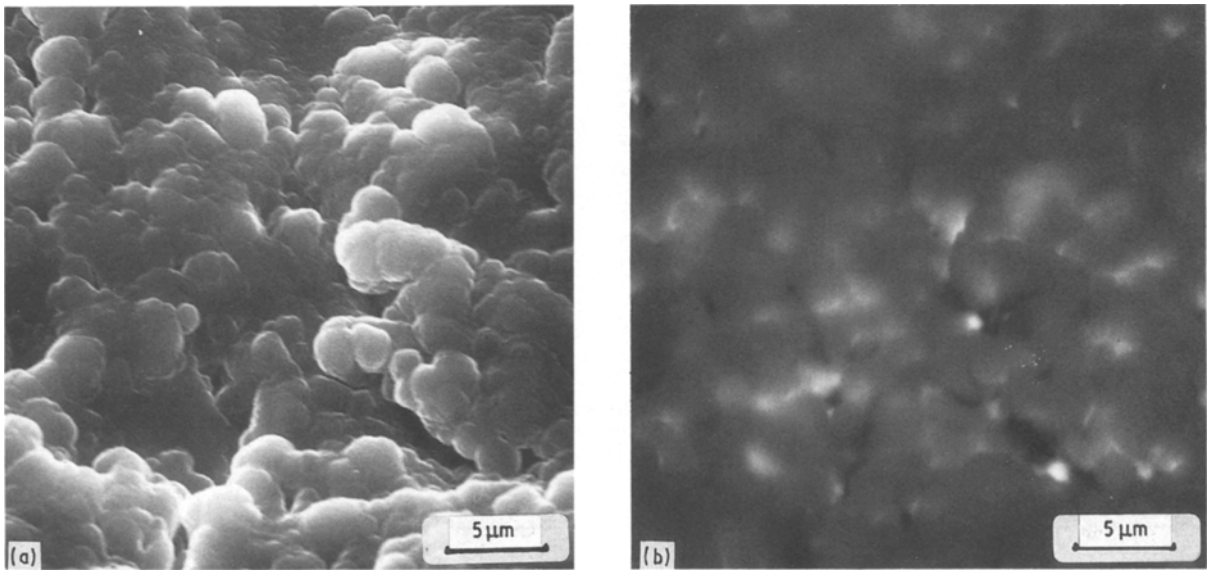

Figure 11 Scanning electron micrographs of the fracture surface of sintered materials from system B: (a) morphology, (b) back-scattered electron image.

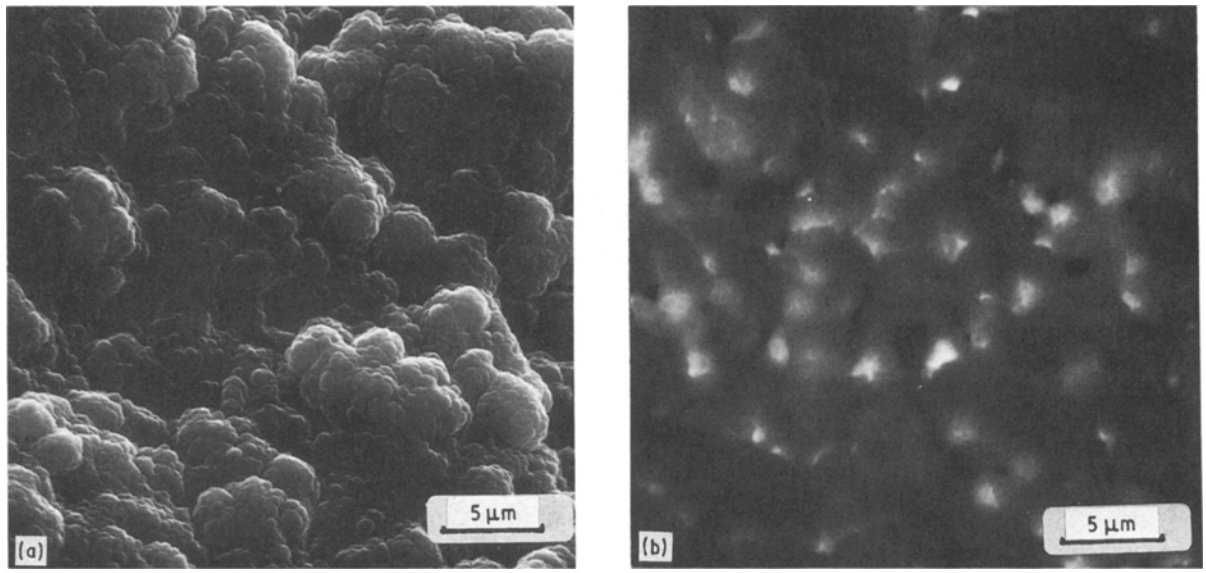

Figure 12 Scanning electron micrographs of the fracture surface of sintered materials from system C: (a) morphology, (b) back-scattered electron image.

transformation is the main toughening mechanism, it can be observed that

(i) the value of K_{IC} is higher in the case of material produced with zirconia powder of low specific surface area, that appears less agglomerated and well distributed. When employing t-ZrO_2 of high specific surface area, the coalescence of ZrO_2 particles seems to play an important role (Fig. 13b) as well as pore size distribution;

(ii) according to fracture mechanics, the strength (S) of a ceramic depends on both K_{IC} and on the critical flaw size (a) (see Table III), i.e. $\sigma = Y(K_{IC}/a^{1/2})$ where Y is a constant that depends on flaw geometry and position. For surface flaws, which are usually the most critical flaws in ceramics, $Y = \pi^{1/2}$ [20]. Therefore, an increase in K_{IC} corresponds to an increase in strength only if the flaw size remains unchanged. Unfortunately, the flaw size changes by changing process and composition of the material.

In our case, the highest strength is obtained for the composite which contains t-ZrO_2 with a high specific surface area, resulting in a well-packed structure without inhomogeneities and defects. The agglomeration of zirconia does not affect the strength, because the cluster size does not exceed 10 μm, a dimension very far from the critical flaw size (see Table III). For ceramics that fail from processing defects, identification of the failure origin is necessary for indicating potential improvement in processing. That is, if a processing defect is identified and its origin assessed, adjustments of the processing procedure should allow further improvements in strength to be made. Fig. 14 compares typical failure origins. For composite A (Fig. 14a), the failure origin is probably related to areas where agglomerates of ZrO_2 and/or Al_2O_3 are present in their immediate vicinity, causing differential sintering. For C (Figs 14b, c), failure origins are predominantly voids both in the form of bubbles under the surface, and in the form of big cracks. As seen in Fig. 14d, the fracture of Al_2O_3 occurs from large grains at or near the tensile surface, resulting in a low value of critical flaw size (Table III). It is clear, when analysing Table III, that the addition of zirconia has significantly increased K_{IC} as a result of transformation toughening (A and B) and of microcracking (C). The behaviour of strength is related to the presence of the critical flaw that resulted from the forming process. Clearly, the removal of these defects would further improve the strength of these materials, and composites of better properties could be produced.

4. Conclusions

Al_2O_3 and Al_2O_3/ZrO_2 powders form stable dispersions in water suitable for producing components by slip casting. With a sufficiently wide powder distribution of the mixtures, a 34 to 50 vol % solids can be achieved, depending on the kind of ZrO_2; the best result was obtained with alumina without additives. Al_2O_3 and Al_2O_3/ZrO_2 composites can be consolidated by slip casting, giving bodies with green densities in the range 54% to 65% of the theoretical density. The powders contain a sufficiently fine colloidal fraction to

TABLE III Some structural parameters and mechanical properties of dense bodies

System	Relative density (%)	ZrO_2 (m)	ZrO_2 (t)	$HV_{0.5}$ (GPa)	K_{IC} (MPa $m^{1/2}$)	Strength (MPa)	Flaw size, a (μm)
A	99.3	10	90	17.1 ± 0.7	5.4	470 ± 45	84
B	98.9	10	90	16.7 ± 0.7	4.2	508 ± 61	41
C	98.6	90	10	12.7 ± 0.7	6.5	192 ± 40	730
D	99.0	–	–	17.6 ± 0.8	3.1	472 ± 44	27

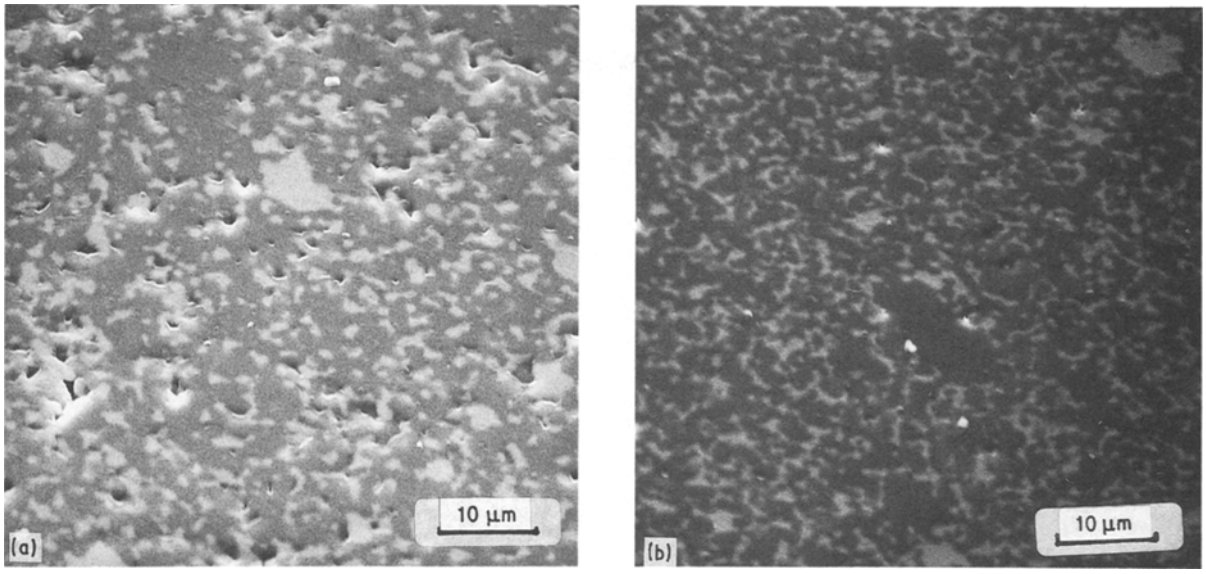

Figure 13 Back-scattered electron images of the polished surfaces of sintered materials from: (a) system C, (b) system A, showing morphology and distribution of ZrO_2 particles and aggregates, and of porosity.

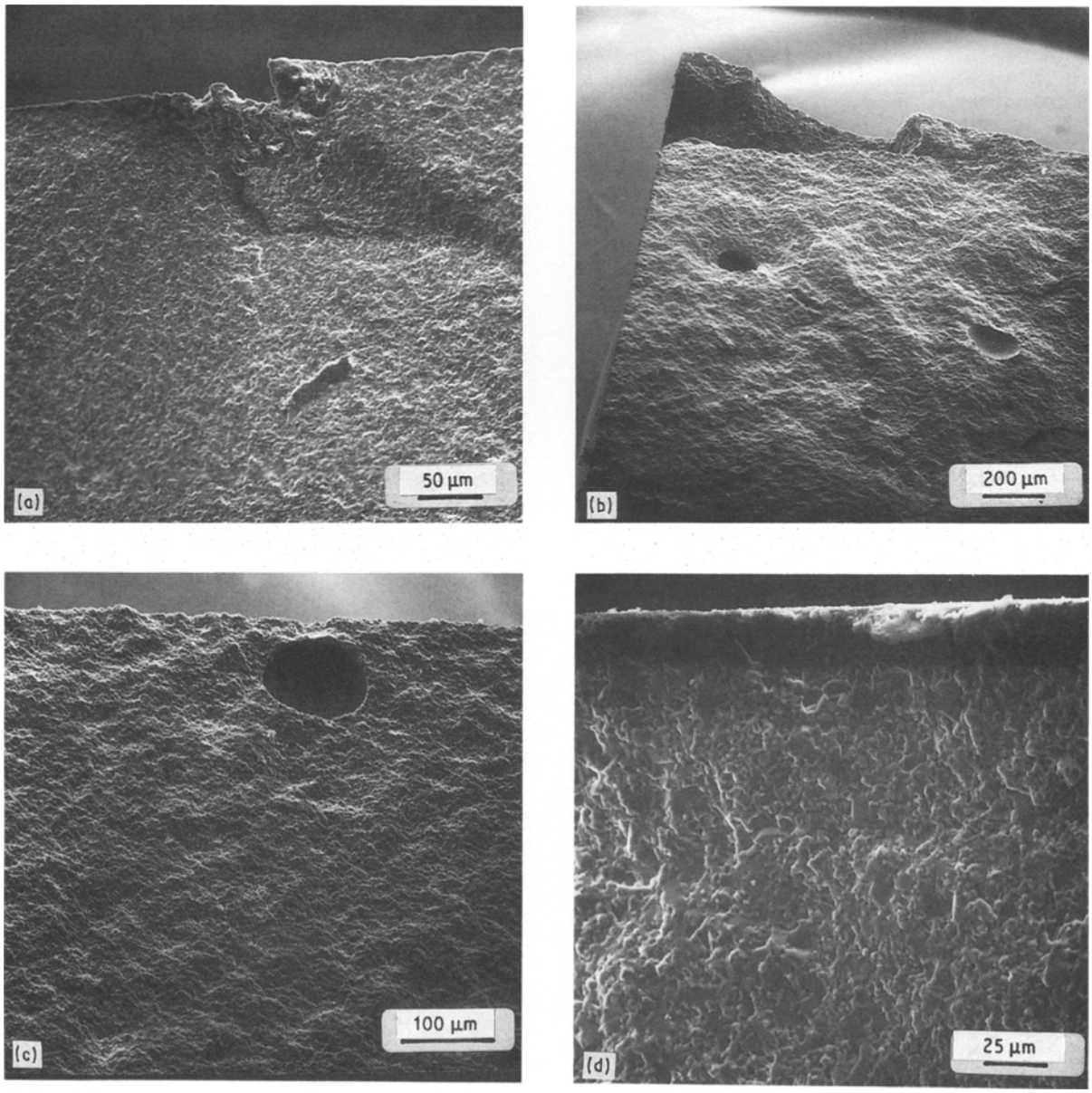

Figure 14 Areas of typical failure origins for the various fabrication routes: (a) system A, (b) system C, (c) system C, (d) system D.

give the slip proper rheological characteristics for casting being a behaviour of shear thinning type. This allows the fabrication of pieces which do not warp during firing. However, the addition of zirconia plays a significant influence both in the presence of defects that affect strength in the fired bodies and in limiting the sintering of Al_2O_3. Alumina was fired to 99% relative density at 1600° C, while higher temperature and soaking time are needed to produce the same density in the composite. The best result (in terms of density and pore size distribution) was achieved with the composite with t-ZrO_2 of low specific surface area (A). The addition of ZrO_2 to Al_2O_3 leads to substantial improvements in fracture toughness, but when m-ZrO_2 is present, microcracking gives rise to a very poor strength. t-ZrO_2, in addition to transformation toughening, can also improve the strength, but it is necessary to optimize the processing route in order to elimnate voids and agglomerates which are the main cause of the failures.

References

1. K. WILFINGER and W. R. CANNON, *Ceram. Engng Sci. Proc.* **9–10** (1986) 1169.
2. E. CARLSTROM and F. F. LANGE, *J. Amer. Ceram. Soc.* **67** (1984) C-169.
3. F. F. LANGE, *ibid.* **66** (1983) 396.
4. F. F. LANGE and M. METCALF, *ibid.* **66** (1983) 398.
5. F. F. LANGE, B. I. DAVIS and I. A. AKSAY, *ibid.* **66** (1983) 407.
6. I. A. AKSAY, F. F. LANGE and B. I. DAVIS, *ibid.* **66** (1983) C-190.
7. N. CLAUSSEN, *ibid.* **59** (1976) 49.
8. *Idem, ibid.* **61** (1978).
9. N. CLAUSSEN, J. STEEB and R. F. PABST, *Amer. Ceram. Soc. Bull.* **56** (1977) 559.
10. T. KOSMAC, M. V. SWAIN and N. CLAUSSEN, *Mater. Sci. Engng* **71** (1985) 57.
11. M. RHULE, N. CLAUSSEN and A. H. HEUER, *J. Amer. Ceram. Soc.* **69** (1986) 195.
12. S. HORI, M. YOSHIMURA and S. SOMYA, *ibid.* **69** (1986) 169.
13. G. DE PORTU, C. FIORI and O. SBAIZERO, "Advances in Ceramics", Vol. 24, "Science and Technology of Zirconia III" (American Ceramic Society, 1988) pp. 1063.
14. A. BELLOSI, C. GALASSI, R. LAPASIN and E. LUCCHINI, in British Ceramic Proceedings, "Novel Ceramic Fabrication Processes and Applications", edited by R. W. Davidge (Institute of Ceramics, Stoke-on-Trent, 1986) pp. 179.
15. N. CELIK, I. E. MELTON and B. RAND, *Trans. J. Brit. Ceram. Soc.* **82** (1983) 136.
16. P. H. DAL and W. J. H. BERDEN, "Science of Ceramics 4" edited by G. H. Stewart (British Ceramic Society, 1963) pp. 113.
17. D. S. ADCOCK and I. C. McDOWALL, *J. Amer. Ceram. Soc.* **40** (1957) 355.
18. A. G. EVANS and E. A. CHARLES, *ibid.* **59** (1976) 371.
19. R. MAJUMDAR, E. GILBART and R. J. BROOK, *Brit. Ceram. Trans. J.* **85** (1986) 156.
20. J. E. RITTER, in "Fracture Mechanics of Ceramics 4", edited by R. C. Bradt, D. P. H. Hasselman and F. F. Lange, (Plenum, New York, London, 1978) pp. 667.

Received 31 May
and accepted 23 October 1989